DISCREPANCIES BETWEEN OBSERVED AND OGCM-SIMULATED ANOMALIES IN RECENT SSTS OF THE TROPICAL INDIAN OCEAN

Goro Yamanaka

Meteorological Research Institute, Email: gyamanak@mri-jma.go.jp

1. INTRODUCTION

It is known that the tropical Indian Ocean (TIO) SSTs have notably increased since the late 20th century ([1]). The TIO warming is considered to contribute to climate impacts by AGCM studies with the prescribed SSTs ([2] [3]). In order to understand the TIO warming mechanism, it is necessary to know the surface heat balance of the Indian Ocean. Since the lack of long-term observation makes it difficult to examine the surface heat balance of the Indian Ocean based on observations, many studies diagnose the surface heat balance by using ocean general circulation model (OGCM) (e.g., [4]). However, current OGCMs give a relatively poor simulation in the Indian Ocean (Fig. 1a), compared to the central to eastern tropical Pacific, and the cause has not been well understood.

The present study examines the cause of the relatively poor simulation of the TIO SSTs ([5]). The knowledge obtained in this study is expected to be useful for ocean modeling studies, as well as for understanding of climatic variability and long-term trends in the Indian Ocean.

2. OGCM AND DATA SETS

The OGCM used in this study is a Meteorological Research Institute community ocean model (MRI.COM, [6]), which is a MOM-type z-coordinate model. The model domain is a near global from 75^{o}S to 75^{o}N. The horizontal resolution is 1^{o} in longitude and 1^{o} in latitude (0.3^{o} near equator). The model has 50 levels in vertical, with 24 levels in the top 200m.

The atmospheric variables as the surface boundary condition are two sets of daily atmospheric reanalysis data: ECMWF 40 years reanalysis data (ERA-40: [7]) and Japan Meteorological Agency 25 years reanalysis data (JRA-25: [8]). The bulk formula for the surface fluxes is based on the formulation by [9]. After the model was integrated for 100 years as spin-up, two experiments (CASE-A and CASE-B) were conducted under different, interannually varying atmospheric forcing data sets (Table 1).

The observed SST data set used here is the COBE-SST data set of in-situ measurements of sea surface temperature ([10]). For comparison with the model results, we used solar radiation and precipitation data derived from JRA-25, ERA-40, in addition to two observation-based estimates: CMAP ([11]) and GPCP ([12]). For comparison among the reanalyses, we also used solar radiation and precipitation data derived from NCEP/NCAR 40-years reanalysis (NCEP1: [13]), and NCEP-DOE AMIP-II reanalysis (NCEP2: [14]), in addition to the ISCCP (International Satellite Cloud Climatology Project) solar radiation data derived from Common Ocean-ice Reference Experiment (CORE/ISCCP: [15]). All data was converted to monthly means before further analysis. Monthly mean data for ERA-40 surface flux was produced by using the daily mean data based on 36 hour forecast data at each 12UTC initials.

3. RESULTS

3.1. Cause of Poor Simulation in the Tropical Indian Ocean

The simulated SST anomaly averaged in the TIO (10^{o}S-10^{o}E, 40^{o}E-100^{o}E) exhibits a trend toward negative values gradually since the late 1990s, which is commonly found in CASE-A (Fig.1b) and CASE-B (not shown). This implies that the poorly simulated SST in the Indian Ocean

Table 1 OGCM Experiments

Experiment Name	*Atmospheric Forcing*	*Integration Period*
CASE-A	*ERA-40*	*1960-2001*
CASE-B	*JRA-25*	*1979-2004*
CASE-C	*ERA-40 but for climatological solar radiation*	*1960-2001*

is the result of the cooling trend, which is inconsistent with the warming trend in the observed SSTs. The sea surface heat fluxes over the TIO in CASE-A display a significant decreasing trend in solar radiation (Fig.1 c).

In order to clarify the role of the reanalyzed solar radiation on the cooling trend in the simulated SSTs, we made an additional experiment (CASE-C), where the atmospheric forcing is the same as CASE-A, except that solar radiation includes only seasonal variations, neither interannual nor longer variations. The simulated SST anomalies in CASE-C display better agreement with the observed than in CASE-A (Fig.1d). It is also found that the TIO warming in the 1990s is roughly captured in CASE-C. The sea surface flux anomalies show that increases in long wave radiation have contributed to the simulated TIO warming in the 1990s in CASE-C (Fig.1e). Reduction of the cooling bias resulted in improved SST simulation skill over the TIO in CASE-C (Fig. 1f). These results strongly suggest that the cooling of the simulated TIO SSTs is primarily caused by the atmospheric reanalysis data used as the surface boundary condition.

3.2. Apparent Trends in Atmospheric Reanalysis Data

Figure 2a shows a time series of precipitation averaged over the TIO derived from the reanalysis data and observation-based estimates. The ERA-40 precipitation data show an increasing trend over the whole period. The JRA-25 precipitation data display a similar increasing trend, though the magnitude of the increase is not as large as that in the ERA-40 data. The observation-based estimates (CMAP and GPCP), in contrast, exhibit no significant increasing trend, so the observed cloud cover presumably does not increase either.

Figure 2b-p show average trends during the period 1979 to 2001 in the atmospheric reanalysis products (JRA-25, ERA-40, NCEP1, and NCEP2) with the prescribed SSTs for the reanalyses, in addition to the

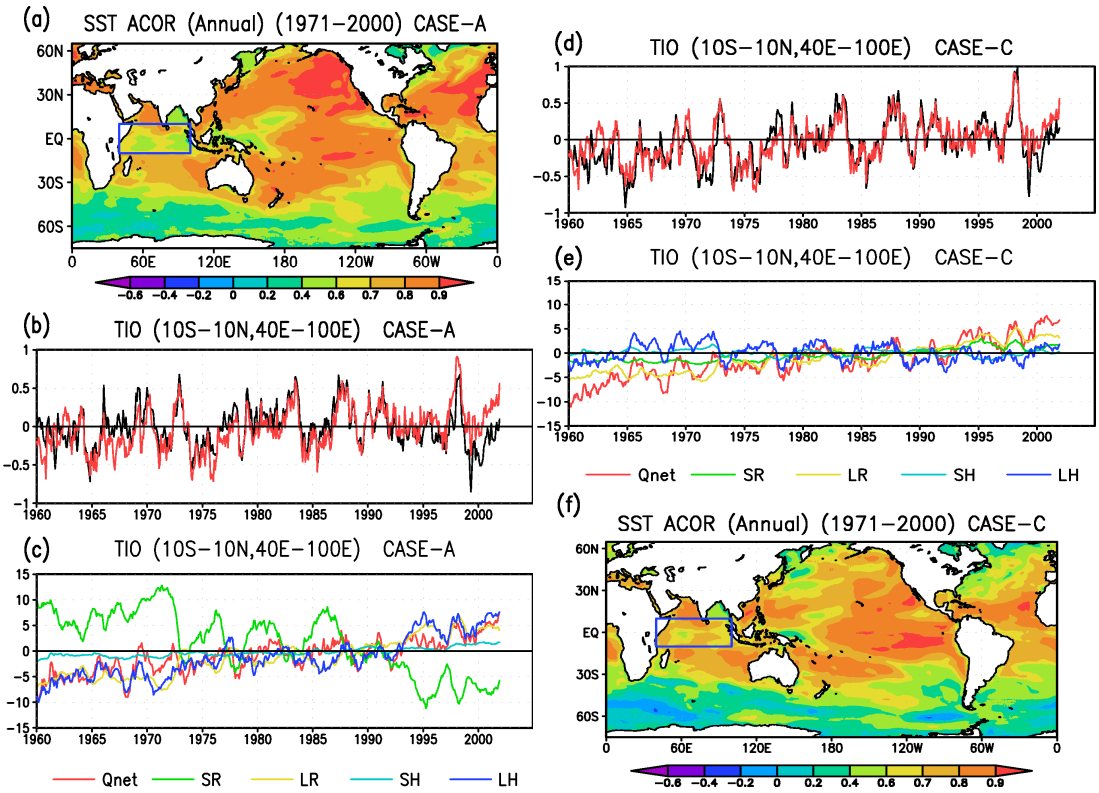

Figure 1: (a) Correlations between annual mean observed and simulated SST anomalies during 1971 to 2000. The OGCM was driven by ERA-40 reanalysis data (CASE-A). The TIO region is denoted by a rectangle. (b) Time series of SST anomalies (^{o}C) averaged over the TIO for CASE-A. Red lines, observed SST anomalies; black lines, simulated SST anomalies. (c) Time series of 13-month running mean surface heat flux anomalies (Wm^{-2}; downward positive) averaged over the TIO for CASE-A. Net surface heat flux (Qnet), solar radiation (SR), long-wave radiation (LR), sensible heat flux (SH), and latent heat flux (LH). (d) Same as (b) except for CASE-C. (e) Same as (c) except for CASE-C. (f) Same as (a) except for CASE-C.

CORE/ISCCP solar radiation and the CMAP precipitation. The reanalysis products exhibit decreasing trends in solar radiation over the Indian Ocean, and their spatial patterns are almost reverse to the precipitation patterns. This feature is generally found in all of the reanalysis products, though it seems more pronounced in JRA25 and ERA40 than in NCEP1 and NCEP2. The increasing trend in precipitation roughly corresponds to the increasing trend in SSTs prescribed as the lower boundary condition for the reanalyses. Hence, it is suggested that the decrease in solar radiation is associated with increases in precipitation directly over the region of most rapidly warming SST. By contrast, an increasing trend in solar radiation over the Indian Ocean is not recognized in the CORE/ISCCP data. Also, the CMAP data shows no increasing trend in precipitation or even a decreasing trend over the southern Indian Ocean.

Several problems in the atmospheric reanalyses may have caused this spurious increasing trend in precipitation. One may come from the bias in the assimilation. For example, it is known that ERA-40 has rainfall problems over tropical oceans from the early 1990s, associated with the bias of satellite radiance corrupted by the Pinatubo eruption ([16]), and that

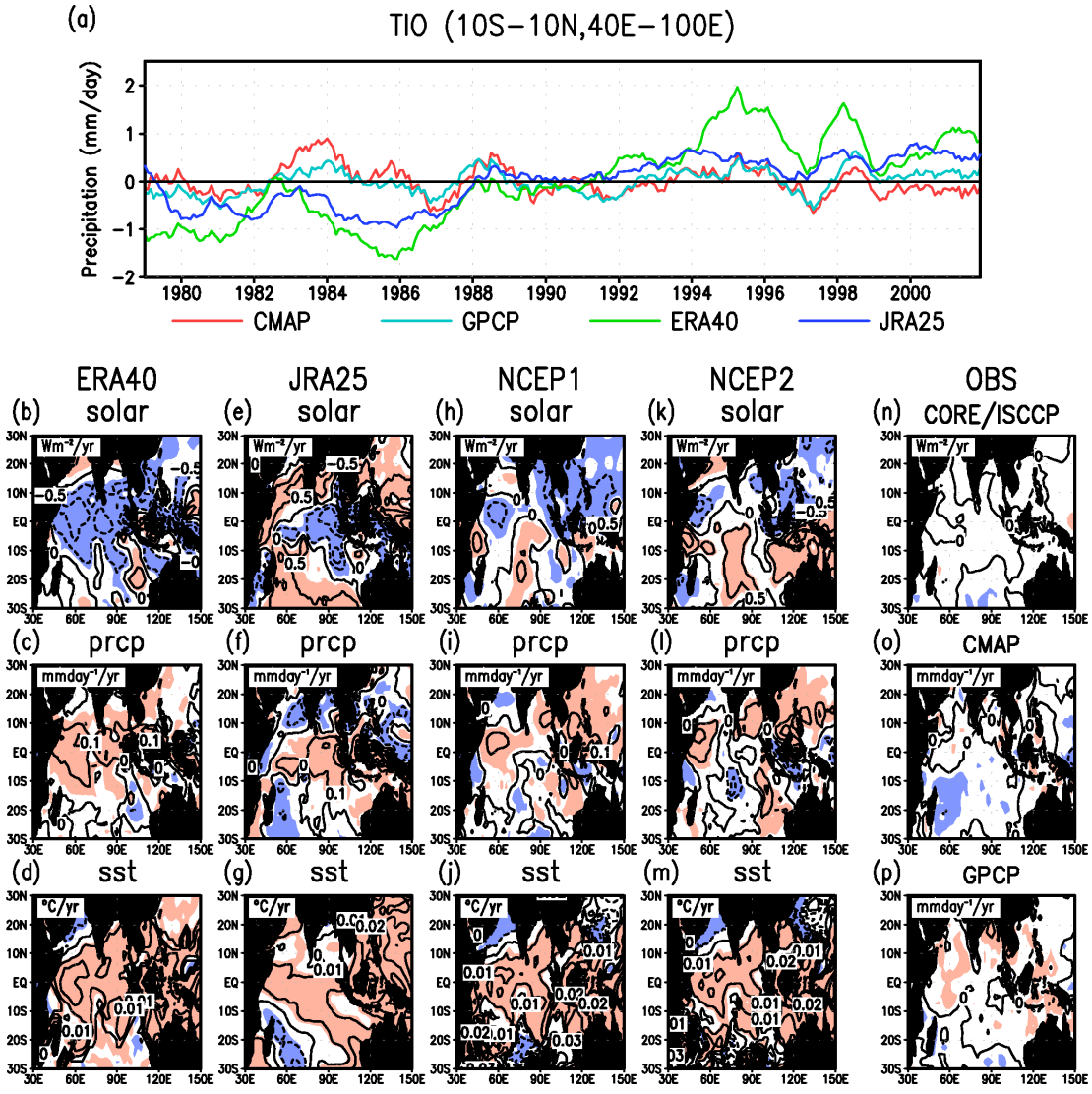

Figure 2: (a) Time series of 13-month running mean precipitation anomalies averaged over the TIO. (b) Columns 1-4: Average trends over the Indian Ocean during 1979 to 2001 in solar radiation (top row) and precipitation (middle row) derived from ERA-40, JRA-25, NCEP1, and NCEP2. The bottom row shows the prescribed SST forcings for the reanalyses. The fifth column shows observed estimates for CORE/ISCCP solar radiation (upper), CMAP precipitation (middle), and GPCP precipitation (lower) for reference. Red and blue shaded areas denote a significant positive and negative rate of change, respectively.

JRA-25 has major discontinuous changes associated with transition from TOVS to ATOVS in November 1998 ([17]). Another may come from the bias in the model. Over tropical oceans where in-situ observations are infrequent and sparse, it is known that a reanalysis dataset would be equivalent to AGCM outputs where SST is given as the lower boundary condition ([18]). Hence, responding to the TIO warming, AGCM tends to enhance convective activities and thus to result in the enhanced increases in precipitation and cloud amount.

As a result, the decrease in the solar radiation caused the cooling trend of the simulated TIO SSTs, inconsistent with the observed SSTs (Fig.1b). This is supported by the fact that the area with a relatively low skill of the simulated SSTs in the TIO approximately corresponds to the area with the decreasing trend in the solar radiation (Fig. 1a). The apparent trends in the atmospheric reanalysis products are a crucial problem especially for long-term OGCM studies. Thus, caution is needed when atmospheric reanalysis data are used to establish surface boundary conditions in OGCMs.

Recently, [19] reported a rise in sea surface pressure, as a proxy for precipitation, over the Indian Ocean between 1950 and 1996. Reference [20] concluded no significant increase in precipitation over the Indian Ocean, based on the analysis of the cloud amount and wind convergence over the ocean. Reference [21] suggests a negative trend in upper level cloud cover in the equatorial Indian Ocean between 1952 and 1997. These findings suggest that no increase or even decreases in precipitation may occur over the Indian Ocean during the second half of the 20th century. Further observation-based studies are needed to elucidate the long-term trend of precipitation in the Indian Ocean. In addition, from the standpoint of ocean modeling, further progress on reanalysis products is desired to improve sea surface fluxes, for example by including air-sea interaction processes (e.g., [22]), which are lacking in the current atmospheric reanalyses.

4. REFERENCES

1. Lau, K.M., & Weng, H.Y. (1999). Interannual, decadal-interdecadal, and global warming signals in sea surface temperature during 1955-97. *J. Climate*, **12**(5), 1257-1267.
2. Hoerling, M.P., Hurrell, J.W. & Xu, T.Y. (2001). Tropical origins for recent North Atlantic climate change. *Science*, **292**(5514), 90-92.
3. Watanabe, M., & Jin, F.-F. (2002). Role of Indian Ocean Warming in the development of Philippine Sea anticyclone during ENSO. *Geophys. Res. Lett*., **29**, 1478, doi:10.1029/2001GL014318.
4. Murtugudde, R., & Busalacchi, A.J. (1999). Interannual variability of the dynamics and thermodynamics of the tropical Indian Ocean. *J. Climate*, **12**, 2300-2326.
5. Yamanaka, G. (2008). Discrepancies between observed and ocean general circulation model-simulated anomalies in recent SSTs of the tropical Indian Ocean caused by apparent trends in atmospheric reanalysis data. *Geophys. Res. Lett.*, **35**, L18603, doi:10.1029/2008GL034737.
6. Ishikawa, I., Tsujino, H., Hirabara, M., Nakano, H., Yasuda, T., & Ishizaki, H. (2005). Meteorological Research Institute Community Ocean Model (MRI.COM) Manual. (in Japanese) Tech. Rep. of Meteorological Research Institute, **47**, 1-189..
7. Uppala, S. M. et al. (2005). The ERA-40 re-analysis, *Q. J. R. Meteorol. Soc.*, **131**, 2961-3012.
8. Onogi, K. et al. (2007). The JRA-25 reanalysis, *J. Meteor. Soc. of Japan*, **85**, 369-432.
9. Kara, A.B., Rochford, P.A., & Hulburt, H.E. (2000). Efficient and accurate bulk parameterizations of air-sea fluxes for use in general circulation models. *J. Atmos. Ocean. Tech.*, **17**, 1421-1438.
10. Ishii, M., Shoji, A., Sugimoto, S., & Matsumoto, T. (2005). Objective Analyses of SST and marine meteorological variables for the 20th Century using ICOADS and the Kobe Collection, *Int. J. Climatol.*, **25**,865-879.
11. Xie, P., & Arkin, P. (1996). Analysis of global monthly precipitation using gauge observations, satellites estimates, and numerical model predictions. *J. Climate*, **9**, 840-858.
12. Adler, R.F. et al. (2003). The version 2 Global Precipitation Climatology Project (GPCP) Monthly Precipitation Analysis (1979-Present), *J. Hydrometeor.*, **4**, 1147-1167.
13. Kalnay, E. et al. (1996). The NCEP/NCAR 40-years reanalysis project, *Bull. Amer. Meteor. Soc.*, **77**,437-471.
14. Kanamitsu, M. et al. (2002). NCEP-DOE AMIP-II reanalysis (R-2), *Bull. Amer. Meteor. Soc.*, **83**,1631-1643.
15. Large, W.G., & Yeager, S.G. (2004). Diurnal to decadal global forcing for ocean and sea-ice models: the data sets and flux climatologies. NCAR Technical Note: NCAR/TN-460+STR.
16. Dee, D., Uppala, S., Kobayashi, S., Lindskog, M., & Simmons, A. (2008). Developments in bias correction for

reanalysis, *Proceedings of the 3rd WCRP International Conference on Reanalysis*, p58.

17. Tsutsui, J., & Kodokura, S. (2008). Multiple regression analysis of the JRA-25 monthly temperature. *Proceedings of the 3rd WCRP International Conference on Reanalysis*, p28.
18. Arakawa, O., & Kitoh, A. (2004). Comparison of local precipitation-SST relationship between the observation and a reanalysis dataset. *Geophys. Res. Lett.*, **31**, L12206, doi:10.1029/2004GL020283.
19. Copsey, D., Sutton, R., & Knight, J. (2006). Recent trends in sea level pressure in the Indian Ocean region. *Geophys. Res. Lett.*, **33**, L19712, doi:10.1029/2006GL027175.
20. Deser, C., & Phillips, A. (2006). Simulation of the 1976/77 climate transition over the North Pacific: Sensitivity to tropical forcing. *J. Climate*, **19**, 6170-6180.
21. Norris, J.R. (2005). Trends in upper-level cloud cover and surface divergence over the tropical Indo-Pacific Ocean between 1952 and 1997. *J. Geophys. Res.*, **110**, D21110, doi:10.1029/2005JD006183.
22. Fujii, Y., Nakaegawa, T., Matsumoto, S., Yasuda, T., Yamanaka, G., & Kamachi, M. (2009). Coupled climate simulation by constraining ocean fields in a coupled model with ocean data, *J. Climate, in press.*